Sensitivity Analysis of Impedance-Based Transmission Line Fault Location Algorithms

Catarina Gaspar, André dos Santos, Maria Teresa Correia de Barros

***Abstract*—A prompt and accurate transmission line fault location is of great interest to transmission system operators (TSOs) as it can accelerate the service restoration, thus reducing outage time and improving service quality. Various transmission lines fault algorithms have been proposed in the past, the impedance-based fault location algorithms being mostly used. This paper is intended to analyze and compare the sensitivity of a single-ended algorithm and a two-ended algorithm, as regards different error sources influencing the algorithms' performance. Both algorithms were implemented in MATLAB. By using EMTP-RV simulations, analysis of the algorithms' sensitivity to: fault resistance, power flow, voltage and current measuring errors, zero-sequence impedance errors and sync errors, is performed (sync errors do not apply for the single-ended algorithm). Results show that the two-ended algorithm is much less sensitive to those sources of errors than the single-ended algorithm, thus being the most suitable for general purpose application in transmission lines fault location. Results obtained with the single-ended algorithm show that it is hugely affected by fault resistance and transmission line zero sequence resistance error. Fault resistance is the factor that most affects the two-ended algorithm for phase-to-ground faults.**

***Index Terms*—Fault location, transmission lines, impedance-based algorithm, single-ended algorithm, two-ended algorithm**

I. Introduction

OVER years, transmission system operators (TSOs) have been pushed towards a continuous improvement of service quality. Hence, accurate transmission line fault location is of great interest as it can accelerate the service restoration, thus reducing outage time and improving system reliability.

Many fault location algorithms have been proposed. These are commonly classified into four distinct categories. (1) impedance-based [1]-[8], (2) travelling waves [9], [10], (3) high frequency [11], and (4) knowledge-based [12], [13].

Impedance-based algorithms are mostly used. They assume that the impedance of a faulted line segment is directly related to fault distance. This category of algorithms can be divided into two main groups: single-ended and two-ended.

The single-ended algorithms make use of voltage and current phasor measurements of only one terminal of the faulted line. The simplest method of this type of algorithms is the simple reactance algorithm [1] which assumes that the fault distance is given by the ratio between the apparent reactance, determined using the phasor measurements, and the line´s reactance, neglecting the fault current. Tagaki et al. [2] proposed a similar method that considers the fault current, however it may be adversely affected by fault resistance. A technique for compensating such effects is described in [3], however more complex also. Since all these methods neglect transversal admittance, in [4] a single-ended method which considers the transversal susceptance is presented.

The two-ended algorithms, as the name suggests, use the two terminals' voltage and current measurements. In [5], a two-ended algorithm utilizing synchronized measurements is presented. An iterative method, which does not require synchronized measurements, is described in [6]. In [7] and [8] non-iterative algorithms adopting unsynchronized two terminal data are presented. While the first requires a synchronization process, the second does not. This limits the first to processing the data offline, while the second, allows location fault being done almost in real time. Moreover, the second algorithm shows little sensitivity to couplings, fault resistance and to the lack of network homogeneity.

Algorithms based on traveling waves [9], [10] utilize propagation and reflection wave theory. When a fault occurs, voltage and current waves propagate from fault's point to line terminals. Given the wave velocity, by measuring the travelling time, it is possible to determine the fault location. These algorithms are quite accurate, but they are complex and expensive, as they require a high sampling frequency.

High frequency algorithms [11] detect and use high frequency voltage and current components, generated by the fault, to determine the fault location. They are also complex and expensive as they need specialized filters to measure the high frequency components, whereby they are not frequently used.

Knowledge-based algorithms are more recent developed to overcome inaccuracies that affect previous methods. Neural network [12] and fuzzy-logic based [13] are examples of this type of algorithms.

M. T. Correia de Barros is with the Department of Electrical and Computer Engineering of Instituto Superior Técnico, Universidade de Lisboa, Portugal (e-mail of corresponding author: teresa.correiadebarros@tecnico.ulisboa.pt.

André dos Santos is with Rede Eléctrica Nacional-REN, Portugal (e-mail: andre.santos@ren.pt).

Catarina Gaspar, now with REN, Portugal, was a Master student at DEEC-IST-Universidade de Lisboa (e-mail: catarina.gaspar@ren.pt).

Paper submitted to the International Conference on Power Systems Transients (IPST2019) in Perpignan, France June 17-20, 2019.

In this paper, two impedance-based algorithms are considered: a single-ended algorithm [2] (see also [14]) and a two-ended algorithm [15], outlined in Section II. They were implemented in MATLAB. Using EMTP-RV, faults of different types were simulated to evaluate the algorithm's sensitivity to several factors. The used methodology is described in section III. Results are presented in section IV. Finally, conclusion is in section V.

II. FAULT LOCATION ALGORITHMS

The two implemented impedance-based fault location algorithms make use of voltage and current measurements and their working principle is based on sequence networks. The transmission line is represented by its per unit length longitudinal positive sequence impedance $\bar{Z}_{l_1}$. Thévenin equivalents of networks upstream from line terminals, S and R, are included. Each one of them is represented by a voltage source, $\bar{U}_S$ and $\bar{U}_R$, respectively, and an equivalent network positive sequence impedance, $\bar{Z}_{S_1}$ and $\bar{Z}_{R_1}$, respectively. The distance to fault, d, seen from terminal S, is to be evaluated by the algorithms.

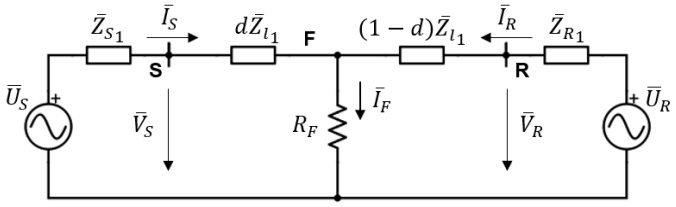

Figure 1 – Single-ended algorithm equivalent circuit.

A. *Single-ended algorithm*

The Tagaki et al. algorithm [2] was implemented (see also [14]). This algorithm uses loop voltages $\bar{V}_{S_l}$ and current $\bar{I}_{S_l}$ computed from measurements at one terminal of the faulted line. The algorithm uses two sets of loop voltages and currents, depending on the fault type. For faults involving the ground, the loop quantities are:

$$\bar{V}_S = \bar{V}_{S_l} = \bar{V}_{S_{ph-n}} \tag{1}$$

$$\bar{I}_S = \bar{I}_{S_l} = \bar{I}_{S_{ph}} - \bar{k}_0 \bar{I}_n \tag{2}$$

where $\bar{V}_{S_{ph-n}}$ is the phase to neutral voltage, $\bar{I}_{S_{ph}}$ the phase current and $\bar{I}_n$ the neutral current. Factor $\bar{k}_0$ is the zero sequence compensation factor given by:

$$\bar{k}_0 = \frac{1}{3}\left(\frac{\bar{Z}_{l_0}}{\bar{Z}_{l_1}} - 1\right) \tag{3}$$

For the other faults, the loop quantities are

$$\bar{V}_{S_l} = \bar{V}_{S_{ph_k - ph_y}} \tag{4}$$

$$\bar{I}_{S_l} = \bar{I}_{S_{ph_k}} - \bar{I}_{S_{ph_y}} \tag{5}$$

where $\bar{V}_{S_{ph_k-ph_y}}$ is the phase to phase voltage, $\bar{I}_{S_{ph_k}}$ and $\bar{I}_{S_{ph_y}}$ being the corresponding phase currents.

Analyzing Figure 1 and according to Kirchhoff laws:

$$\bar{V}_S = d\bar{Z}_{l_1}\bar{I}_S + R_F\bar{I}_F \tag{6}$$

$$\bar{I}_F = \bar{I}_S + \bar{I}_R \tag{7}$$

Both current $\bar{I}_R$ and $\bar{I}_F$ are unknown, thus making it impossible to determine the fault distance, d, from (6).

One way to overcome this problem is to assume that the fault current $\bar{I}_F$ is proportional to the current variation at point S when the fault occurs:

$$\bar{I}_S - \bar{I}_{S0} \equiv \Delta\bar{I}_S = k_d\bar{I}_F \tag{8}$$

where $\bar{I}_{S0}$ is the pre-fault current at point S and k_d is the distribution factor, given by (9), obtained by the Superposition Theorem, considering the contributions of both line-ends to the fault current.

$$k_d = \frac{\bar{Z}_{R_1} + (1-\mathrm{d})\,\bar{Z}_{l_1}}{\bar{Z}_{R_1} + \bar{Z}_{S_1} + \bar{Z}_{l_1}} \tag{9}$$

For low values of R_F, the pre-fault current being negligible as compared to the fault current, it was demonstrated in [2] that k_d is approximately equal to 1. For higher values of R_F, the computed distance becomes insensitive to the value of k_d , and it can be also assumed equal to 1. Therefore, by replacing (8) in (6):

$$\bar{V}_S = d\bar{Z}_{l_1}\bar{I}_S + R_F(\bar{I}_S - \bar{I}_{S0}) \tag{10}$$

Equation (10) involving complex quantities, it can be separated into its real and imaginary parts, thus obtaining a system of two linear equations, allowing to compute the two unknown variables, d and R_F:

$$\begin{cases} Real\{\bar{V}_S\} = d \times Real\{\bar{Z}_{l_1}\bar{I}_S\} + R_F \times Real\{(\bar{I}_S - \bar{I}_{S0})\} \\ Imag\{\bar{V}_S\} = d \times Imag\{\bar{Z}_{l_1}\bar{I}_S\} + R_F \times Imag\{(\bar{I}_S - \bar{I}_{S0})\} \end{cases} \tag{11}$$

B. *Two-ended algorithm*

The implemented algorithm is a simplified version of the phasor-based approach of fault location with use of two-end synchronised measurements [15] (transmission lines were represented by the longitudinal impedance). This algorithm uses positive sequence voltages and currents at both terminals of the faulted line. Figure 1 is also applicable, all voltages and currents being the positive sequence components of the corresponding measured quantities:

$$\bar{V}_S = \bar{V}_{S_1}, \bar{I}_S = \bar{I}_{S_1} \tag{12}$$

$$\bar{V}_R = \bar{V}_{R_1}, \bar{I}_R = \bar{I}_{R_1} \tag{13}$$

The resistive branch R_F is now replaced by the positive sequence fault voltage $\bar{V}_{F_1}$, this depending on the fault type. From Figure 1 and according to Kirchhoff law:

$$\bar{V}_S = d\bar{Z}_{l_1}\bar{I}_S + \bar{V}_{F_1} \tag{14}$$

$$\bar{V}_R = (1-d)\bar{Z}_{l_1}\bar{I}_R + \bar{V}_{F_1} \tag{15}$$

From (6) and (14), one can obtain two equations for $\bar{V}_F$:

$$\bar{V}_F = \bar{V}_S - d\bar{Z}_{l_1}\bar{I}_S \quad (16)$$

$$\bar{V}_F = \bar{V}_R - (1-d)\bar{Z}_{l_1}\bar{I}_R \quad (17)$$

Finally, from (16) and (17), the fault distance d is given by:

$$d = \frac{\bar{V}_S - \bar{V}_R + \bar{Z}_{l_1}\bar{I}_R}{\bar{Z}_{l_1}(\bar{I}_S + \bar{I}_R)} \quad (18)$$

III. Methodology for the Sensitivity Analysis

To test both algorithms and their sensitivity to several factors, the test network, represented in Figure 2, was configured in EMTP-RV. Various types of faults were forced in two different transmission lines: TL 1-2 connecting Substation 1 to Substation 2, and TL 2-3, connecting Substation 2 to Substation 3. The simulated faults are: *single phase-to-ground*, *phase-to-phase*, *double phase-to-ground*, and *three-phase* faults. Faults were simulated at different given distance from the line ends. For faults involving the ground, six different ground fault resistances were considered: 0 Ω, 10 Ω, 20 Ω, 30 Ω, 40 Ω, and 50 Ω. For all simulations, five different pre-fault scenarios were also considered, by means of changing the angle between the Thévenin voltage sources: -10 º, -5 º, 0 º, 5 º and 10 º. Table 1 shows the corresponding active power values.

Table 1 – Pre-fault scenarios

Angle between Thévenin voltage sources	Active power [MW]	
	TL 1-2	TL 2-3
-10 º	163.89	8.47
-5 º	95.84	5.10
0 º	21.84	1.05
5 º	-56.92	-3.57
10 º	-139.18	-8.62

Because errors related to voltage and current measurements, zero sequence impedance and synchronization may also affect the algorithms performance, with respect to estimated distance, these factors were also considered. Regarding current measurements errors, amplitude ($|\bar{I}|$) errors of -5, -3, -1, 0, 1, 3, and 5 % were considered, according to [16]. Regarding voltage measurements errors, amplitude ($|\bar{V}|$) and angle ($\measuredangle\bar{V}$) errors of: {-3; -2; -1; 0; 1; 2; 3} %, and {-2; -1.2; -0.4; 0; 0.4; 1.2; 2} º were respectively considered, according to [17]. For zero sequence impedance errors, zero sequence resistance (R_h) and reactance (X_h) of {0.9004; 1; 1.1503; 1.4002; 1.6501; 1.9} pu and {0.9462; 0.9925; 1; 1.0388; 1.0851} pu, respectively, were considered, according to [18]. Regarding sync errors, {-2; -1.2; -0.4; 0; 0.4; 1.2; 2} ms of phase shift between the measurements of line-terminals S and R were considered. Sync errors do not apply for the single-ended algorithm.

Results were obtained by applying the simulations in the two implemented algorithms, and algorithms sensitivity analysis to: fault resistance, power flow, voltage and current measuring errors, zero-sequence impedance errors and sync errors, was performed.

For each type of fault and algorithm, the estimated distance error was computed:

$$\varepsilon\ (\%) = \frac{d_{algorithm} - d_{real}}{d_{real}} \times 100 \quad (19)$$

where $d_{algorithm}$ is the fault distance estimated by the algorithm and d_{real} is the simulated fault distance. Knowing this, the largest error observed, regarding only each factor, is the maximum of $\Delta\varepsilon$ observed, where $\Delta\varepsilon$ is given by:

$$\Delta\varepsilon(\%) = |\varepsilon\ (\%) - \varepsilon_0\ (\%)| \quad (20)$$

where ε_0 is the $error$ obtained for 0 % error of each factor considered. For the resistance and power flow, ε_0 corresponds to the results obtained with 0 Ω and 0 º, respectively.

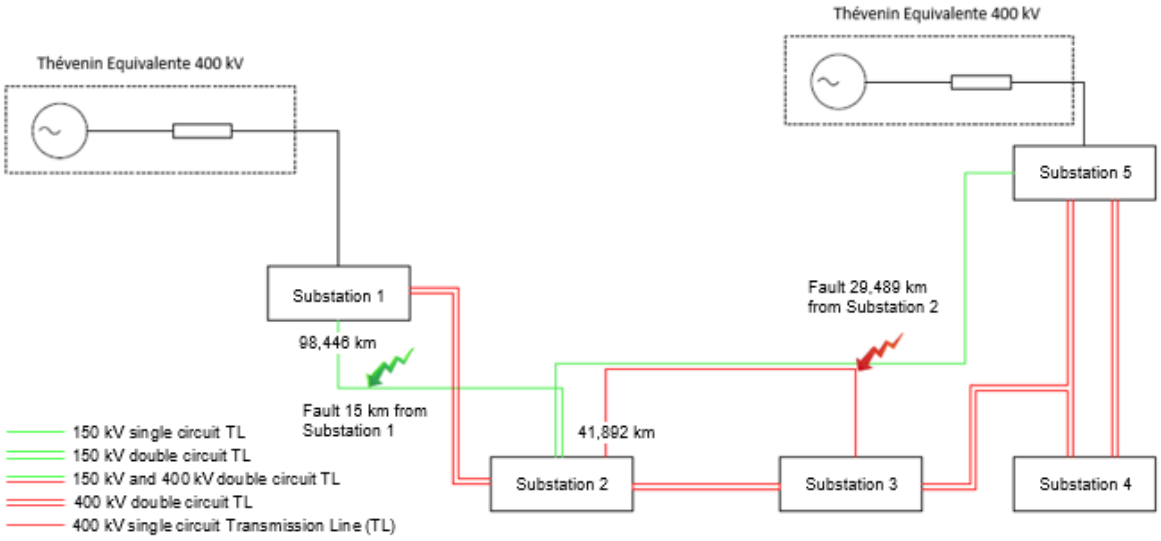

Figure 2 – Test Network.

IV. RESULTS

Results were translated into bar charts, so to emphasize the relative importance of each factor: fault resistance (R_F), power flow (PF), current amplitude ($|\bar{I}|$) and voltage amplitude ($|\bar{V}|$) errors, voltage angle errors ($\measuredangle\bar{V}$), zero sequence resistance (R_h) and reactance (X_h) errors, and sync errors (Sync).

Notice that the presented results do not allow evaluating the total error of the fault location algorithm in estimating the distance to fault. Indeed, this error is not the sum of the presented values of the individual errors, as some factors will contribute positively and others negatively to the global error.

A. Single Phase-to-ground faults

The bar chart mentioned above for phase-to-ground faults is presented in Figure 3.

Results show that the two-ended algorithm is much less sensitive than the single-ended algorithm, for every single factor considered (please note the different yy-scales).

The three factors that hugely affect the estimated fault distance errors obtained with the single-ended algorithm are: (1) zero sequence resistance errors, (2) fault resistance value, and (3) voltage angle measurement errors. The zero sequence resistance error originates a maximum 105% error in the distance to fault evaluation. The errors associated to the fault resistance value reaches 88% for a 50 Ω fault resistance, this being the higher fault resistance value considered. This result should be expected as these two errors are directly related to the algorithm assumption of considering the distribution factor, k_d equal to 1, and this is only acceptable for low fault resistance values. The third mostly affecting factor is the voltage angle measurement error, the maximum observed $\Delta\varepsilon$ being less than 32 %.

Results for the two-ended algorithm show that this algorithm is mostly affected by the fault resistance value, sync errors and current amplitude measurement errors. The corresponding associated errors less than 10 % for the first and around 3 %, for the two others.

Results in Figure 3 also show that the two-ended algorithm is non-sensitive to zero sequence impedance errors. This should be expected since this algorithm does not use zero sequence quantities in its calculations. Accordingly, for this algorithm, zero sequence resistance and reactance errors were not performed for the faults that follow.

B. Phase-to-phase faults

Figure 4 presents results for phase-to-phase faults.

Results show that the two-ended algorithm is again less sensitive than the single-ended algorithm, for every single factor considered. For this type of faults, current and voltage amplitude measurements errors are the factors that most affect both algorithms.

For the single-ended algorithm, results for $\Delta\varepsilon$ were all less than 6.2 % and 2.9 % regarding current and voltage amplitude errors, respectively. On the other hand, these values for the two-ended algorithm are lower than 2.6 % and 1.2 %, respectively.

It is also important to mention that, for this type of faults, the single-ended algorithm is not sensitive to zero impedance errors. This is explained by the fact that, for this type of fault, the algorithm does not make use zero sequence quantities.

C. Double phase-to-ground faults

Figure 5 presents results for double phase-to-ground faults.

Again, results show that the two-ended algorithm is less sensitive than the single-ended algorithm, for every single factor considered.

For this type of faults, current and voltage amplitude measurements errors are still the factors that most affect both algorithms. Results of single-ended algorithm showed $\Delta\varepsilon$ less than 4.9 % and 2.9 %, respectively for the current and voltage errors. On the other side, the two-ended algorithm showed $\Delta\varepsilon$ less than 2 % and 1.2 %, respectively.

Furthermore, fault resistance value is one of the factors that also significantly affects the algorithms' performance. However, both algorithms showed much lower errors than the ones for phase-to-ground faults. Indeed, for double phase-to-ground faults, the single-ended and two-ended algorithms showed a maximum $\Delta\varepsilon$ of 0.65 % and 1.27 %, respectively, while for phase-to-ground faults the corresponding errors were 87.7, % and 9.83 %, respectively.

D. Three-phase faults

Figure 6 presents the results obtained for three-phase faults.

Results show that the two-ended algorithm is once again less sensitive than the single-ended algorithm, for every single factor considered.

Once again, current and voltage amplitude measurements errors are the ones that most affect both algorithms for three-phase faults. For this case, 5.6 % and 3.17 % are the maximum $\Delta\varepsilon$ values obtained for the single-ended algorithm for current and voltage amplitude measurement errors. For the two-ended algorithm, these values are 1.87 % and 1.08 %, respectively.

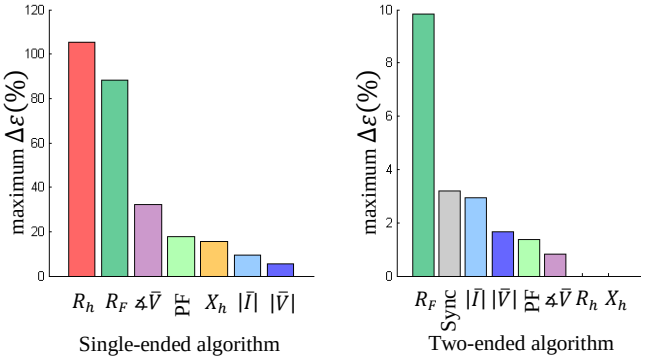

Figure 3 – Sensitivity analysis for single phase-to-ground faults.

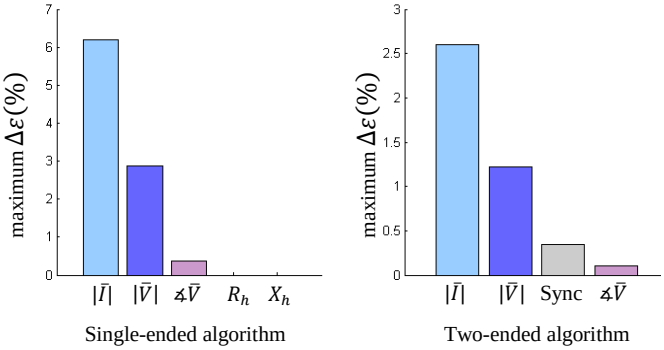

Figure 4 – Sensitivity analysis for phase-to-phase faults.

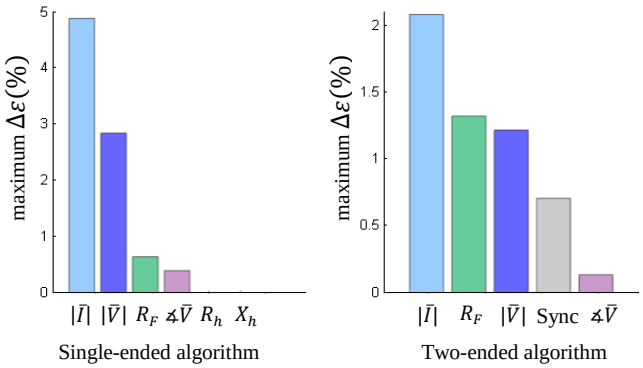

Figure 5 – Sensitivity analysis for double phase-to-ground faults.

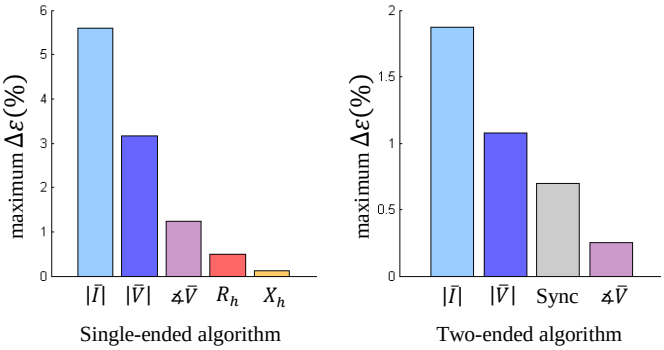

Figure 6 – Sensitivity analysis for three-phase faults.

V. Conclusion

Two impedance-based fault location algorithms were implemented: a single-ended algorithm and a two-ended algorithm.

Sensitivity analyzes regarding: (1) fault resistance value, (2) pre-fault conditions, (3) current and voltage measurement errors, (4) zero sequence impedance errors, and (5) sync errors were performed for the two implemented algorithms, using EMTP-RV simulations. The sync errors sensitive analysis is only applicable to the two-ended algorithm.

The sensitivity analyses were performed for single phase-to-ground, phase-to-phase, double phase-to-ground, and three-phase faults. The values of the above-mentioned parameters were varied in a realistic range.

Results show that the two-ended algorithm is much less sensitive to the considered factors than the single-ended algorithm, for every fault type.

Results also show that the fault location error depends on the fault type, being higher for phase-to-ground faults.

For every individual factor evaluated, the two-ended algorithm showed errors below 10 %, for all types of fault, thus being most suitable for general purpose application. The highest error corresponds to the considered fault resistance value of 50 Ω for the phase-to-ground fault.

For the single-ended algorithm, it was shown that it is very sensitive either to the zero sequence resistance error, the fault resistance value and the voltage angle measurement error, showing errors that can go up to 105 %, 88 % and 32 %, for each individual factor respectively, for phase-to-ground faults.

VI. Acknowledgement

The authors thank PowerSys Solutions for offering partnership to IST-Universidade de Lisboa, kindly providing the EMTP-RV software used in the presented work.

References

[1] K. Zimmerman and D. Costello, “Impedance-based fault location experience”, in *2005 58th Annual Conference for Protective Relay Engineers*, College Station, TX, USA, 2005

[2] T. Takagi, Y. Yamakoshi, M. Yamaura, R. Kondow, and T. Matsushima, “Development of a new type fault locator using the One-Terminal voltage and current data,” *IEEE Power Eng. Rev.*, vol. PAS-101, no. 8, pp. 2892–2898, 1982

[3] L. Erikson, M. M. Saha, and G. D. Rockefeller, “An accurate fault locator with compensation for apparent reactance in the fault resistance resulting from remote-end infeed,” *IEEE Trans. Power Appar. Syst.*, vol. PAS-104, no. 2, pp. 423–436, 1985

[4] J. Izykowski, E. Rosolowski, and M. M. Saha, “Locating faults in parallel transmission lines under availability of complete measurements at one end,” *IEE Proc. - Gener. Transm. Distrib.*, vol. 151, no. 2, pp. 268–273, 2004

[5] T. Johns and S. Jamali, “Accurate fault location technique for power transmission lines,” *IEE Proc. C - Gener. Transm. Distrib.*, vol. 137, no. 6, pp. 395–402, 1990

[6] A. A. Girgis, D. G. Hart, and W. L. Peterson, “A New Fault Location Technique for Two- and Three-Terminal Lines,” *IEEE Trans. Power Deliv.*, vol. 7, no. 1, pp. 98–107, 1992

[7] J. Izykowski, E. Rosolowski, P. Balcerek, M. Fulczyk, and M. M. Saha, “Accurate noniterative fault-location algorithm utilizing two-end unsynchronized measurements,” *IEEE Trans. Power Deliv.*, vol. 26, no. 2, pp. 547–555, 2011

[8] D. A. Tziouvaras, J. Roberts, and G. Benmouyal, “New Multi-ended fault location design for two- or three-terminal lines,” in *Developments in Power System Protection, Seventh International Conference on (IEE)*, no. 479, pp. 395–398, Amsterdam, 2001

[9] F. H. Magnago and A. Abur, “Fault Location Using Wavelets,” *IEEE Trans. Power Deliv.*, vol. 13, no. 4, pp. 1475–1480, 1998

[10] D. Wenjin, F. Min, and C. Lizhen, “Traveling wave fault location system,” Proc. World Congr. Intell. Control Autom., vol. 2, pp. 7449–7452, 2006.

[11] Z. Q. Bo, G. Weller, and M. A. Redfern, “Accurate fault location technique for distribution system using fault-generated high-frequency transient voltage signals,” *IEE Proc. - Gener. Transm. Distrib.*, vol. 146, no. 1, pp. 73–79, 1999

[12] R. Mahanty and P. Gupta, “Application of RBF neural network to fault classification and location in transmission lines,” IEE Proceedings-Generation, Transm. …, vol. 151, no. 3, pp. 201–212, 3900.

[13] M. Jayabharata Reddy and D. K. Mohanta, “A wavelet-fuzzy combined approach for classification and location of transmission line faults,” *Electr. Power Energy Syst.*, vol. 29, no. 9, pp. 669–678, 2007

[14] S. H. Horowitz, A. G. Padhke, “Power System Relaying”, 4th edition, Wiley, pp. 311-316.

[15] J. Iżykowski, *Fault location on power transmission lines*, Oficyna Wydawnicza Politechniki, Wrocław, 2008

[16] *Instrument transformers - Part 2: Additional requirements for current transformers*, IEC 61869 2, 2012

[17] *Instrument transformers - Part 3: Additional requirements for inductive voltage transformers*, IEC 61869 3, 2011

[18] A. Dos Santos and M. T. Correia de Barros, “Transmission Line Zero Sequence Impedance Probabilistic Model - effect of the earth resistivity uncertainty”, in *CAGRE 2015 Algerian Large Electrical Network Conference*, No 15, 2015.